

Realizing the canonical ensemble in highly entropic inhomogeneous materials

B. Joós* and Z. Zhou†

Ottawa Carleton Institute of Physics, University of Ottawa Campus, Ottawa, Ontario, Canada K1N-6N5

(Received 19 July 1999)

To properly model highly entropic inhomogeneous materials in the canonical ensemble by molecular dynamics simulations, it is necessary to choose algorithms which rigorously implement the ensemble. Approximate methods may have either very low efficiency or completely fail in the very soft regime. The calculation of the shear modulus of the diluted central force network is used to illustrate this point. Four algorithms to realize the canonical ensemble have been tested on two methods of evaluation of the shear modulus.

PACS number(s): 65.50.+m, 02.70.Ns, 61.43.-j, 62.20.Dc

I. INTRODUCTION

The canonical ensemble is the most commonly used ensemble in the study of the equilibrium properties of materials. To realize it efficiently and correctly in computer simulations is therefore an important issue. A number of algorithms simulating, either rigorously or approximately, the canonical ensemble by molecular dynamics (MD) simulations have been successfully applied to liquids and solids [1–13]. Despite the existence of the rigorous methods [4,10–12] approximate methods are still widely used because of their simplicity and speed. In general they yield the same results within statistical error as the rigorous methods. However, whether this equivalence still holds for the inhomogeneous soft systems is not clear. Soft inhomogeneous materials, such as crosslinked polymer melts, present particular challenges to the simulation algorithms [14]. In a recent paper [15] we reported that the usual criteria for the choice of the time step, the stability of the energy and the pressure, are not always appropriate in the study of highly entropic materials. In this paper we further confirm this point and investigate the appropriateness for these systems of several well accepted algorithms. Some of these have very low efficiency or even completely fail for soft materials.

The system studied is a two-dimensional (2D) diluted central force network (DCFN) near its percolation threshold. We focus on the shear modulus which characterizes the rigidity of the system. The shear modulus was calculated using two different methods. In the stress-strain method (SSM) the shear modulus is obtained from the changes in the stress (or pressure) tensor upon deformation. We call this a macroscopic measurement and label it μ_{ss} . In contrast, in the equilibrium fluctuation method (EFM), the shear modulus is extracted from the microscopic fluctuations in the system. We label this second measurement μ_{ef} . The efficiency of the different MD algorithms will be investigated by comparing the agreement between μ_{ss} and μ_{ef} . Four different MD algorithms for the canonical ensemble are studied. They are the velocity rescaling algorithm (labeled A), the damped

force algorithm (B), the rigorous Brownian dynamics algorithm (C), and the approximate Brownian dynamics algorithm (D). Of the four algorithms, only C generates a rigorous canonical ensemble. It is the only algorithm that can be applied successfully to all regimes, from the perfect rigid lattice to the very soft diluted lattice just above the percolation threshold. In contrast, the different approximate methods work properly only in relatively rigid lattices.

The paper is organized as follows. After a brief introduction to the four MD algorithms for the canonical ensemble in Sec. II, Sec. III, and Sec. IV describe respectively the methods to calculate the shear modulus and the model studied. In Sec. V we present the results and follow up with a discussion and conclusion in Sec. VI.

II. ALGORITHMS TO REALIZE THE CANONICAL ENSEMBLE

We present here briefly the algorithms used in this work to realize the canonical ensembles.

A. Algorithm A: The rescaling of velocities

The simplest way to construct an approximate canonical ensemble is to scale the velocities at every time step to keep the total kinetic energy constant in accordance with the required temperature T . The velocity Verlet algorithm [12] is used to integrate the Newton's equations of motion in this work.

B. Algorithm B: The damped force algorithm

Another simple way to yield an approximate canonical ensemble is the damped force method [6,7]. It involves the integration of a set of Hamiltonian equations of motion

$$\begin{aligned} \frac{d\mathbf{x}_i}{dt} &= \frac{\mathbf{p}_i}{m_i}, \\ \frac{d\mathbf{p}_i}{dt} &= -\frac{\partial\Phi}{\partial\mathbf{x}_i} - \frac{\alpha\mathbf{p}_i}{m_i}, \end{aligned} \quad (2.1)$$

where m_i is the mass of the particle, Φ is the interparticle interaction potential, α is the damping factor determined by requiring that $dT_{\text{int}}/dt=0$, i.e., keeping the instantaneous temperature T_{int} constant. With

*Electronic address: bjoos@physics.uottawa.ca.

†Present address: Department of Physics, National Central University, Chung-Li, Taiwan 32054. Electronic address: zzhou@spl1.phy.ncu.edu.tw

$$T_{\text{int}} = \frac{1}{(dN-d-1)k_B} \sum_{i=1}^N \frac{p_i^2}{m_i}, \quad (2.2)$$

where N is the number of particles, d the dimension of the system,

$$\alpha = \frac{\sum_{i=1}^N m_i \mathbf{F}_i \cdot \mathbf{p}_i}{N \sum_{i=1}^N p_i^2}, \quad (2.3)$$

where $\mathbf{F}_i = -\partial\Phi/\partial\mathbf{x}_i$ is the force on particle i . Note that α is not a constant. This method yields a distribution of states in phase space [7,12]

$$P(\mathbf{r}, \mathbf{p}) \propto \delta(T_{\text{int}} - T) \delta(\mathbf{P}) \exp\left(\frac{-\Phi}{k_B T}\right), \quad (2.4)$$

where \mathbf{P} is the total linear momentum. Therefore, this method generates configurational properties in the canonical ensemble. The momentum distribution is, however, not canonical, but it was believed that the equivalence of ensembles guarantees that the differences in most averages will be of the order of $\mathcal{O}(1/N)$ [12]. This may not be true for response functions. The ‘‘leapfrog’’ Verlet algorithm [12,16] was used to integrate the equations of motion in this work. At small time step, this method should be equivalent to the method of the rescaling of velocities [12].

C. Algorithm C: The rigorous Brownian dynamics algorithm

The principle of the Brownian dynamics algorithm [3,12] is to integrate the following equation of motion for each particle i :

$$m_i \frac{d^2 \mathbf{x}_i}{dt^2} = -\frac{\partial\Phi}{\partial\mathbf{x}_i} - m_i \Gamma \frac{d\mathbf{x}_i}{dt} + \mathbf{W}_i(t), \quad (2.5)$$

where the friction parameter Γ and the random noise term $\mathbf{W}_i(t)$ couple the system to a heat bath. The random force acts on each particle and is related to the friction by the fluctuation dissipation theorem

$$\begin{aligned} \langle \mathbf{W}_i(t) \cdot \mathbf{W}_j(t') \rangle &= 2 dk_B T \Gamma \delta_{ij} \delta(t-t'), \\ \langle \mathbf{W}_i(t) \rangle &= \mathbf{0}, \end{aligned} \quad (2.6)$$

Γ is related to the diffusion coefficient D by $\Gamma = k_B T / mD$ and is irrelevant for static properties. We used $\Gamma = 0.5$ for almost all of our work. $\mathbf{W}_i(t)$ is specified by a Gaussian distribution [12]. This method yields a rigorous canonical ensemble [12].

D. Algorithm D: The approximate Brownian dynamics algorithm

To implement the Gaussian distribution is time consuming. For a rigid system, the Gaussian distribution can be

replaced by a uniform random number distribution without affecting some properties [17]. However, as we will report, such an approximation does not work well in the soft regime because of ergodicity breaking.

III. CALCULATION OF THE SHEAR MODULUS

Here is a brief description of the two methods used to obtain the elastic constant for pure shear deformation. This is an area preserving deformation, where the system is elongated in one direction, and appropriately compressed in the other direction. The formulas are specifically written for the 2D system. The first method is the stress-strain method (SSM). The modulus for pure shear is obtained from the changes in the applied stress tensor $S_{\alpha\beta}$ (negative for compression) under a strain represented by the Lagrangian strain tensor η [15,18]

$$\mu_{ss} \equiv \frac{S_{11}(\eta) - S_{22}(\eta) - [S_{11}(0) - S_{22}(0)]}{4 \eta_{11}}. \quad (3.1)$$

Note that Eq. (3.1) requires $S_{\alpha\beta}(0)$ which may be anisotropic. What is actually calculated is

$$\mu_{ss} \equiv \frac{S_{11}(\eta) - S_{22}(\eta)}{4 \eta_{11}}, \quad (3.2)$$

which assumes that $S_{\alpha\beta}(0) = 0$. The off-diagonal elements of $S_{\alpha\beta}(0)$ are small and of no concern. There are, however, due to finite size effects, non-negligible diagonal elements $S_{\alpha\alpha}(0)$. The simplest way to eliminate these frozen-in stresses in the undeformed sample is to perform the deformation of every sample in the two Cartesian directions in turn, as we did in this work. The deformation of a sample in one Cartesian direction is therefore called a realization and every sample yields two realizations.

The second method is the equilibrium fluctuation method (EFM) which calculates directly the elastic constants from the microscopic fluctuations of the system over time without the need to impose deformations. All elastic constants are obtained from a single run. Note that within the linear stress-strain regime, elastic constants should be basically constants and therefore deformed and undeformed states yield the same results. This property greatly simplifies the comparison between the two methods since we can calculate both μ_{ef} and μ_{ss} simultaneously in a deformed state as we did for most samples in this work. In this method, the modulus μ_{ef} for pure shear for a 2D system is given by [14]

$$\mu_{ef} = \frac{c_{11} + c_{22} - c_{12} - c_{21}}{4} \quad (3.3)$$

where $c_{\alpha\beta}$ are the condensed Voigt notation of elastic stiffness coefficients [19,20] defined by

$$S_{\alpha\beta}(\eta) = S_{\alpha\beta}(0) + c_{\alpha\beta\sigma\tau} \eta_{\sigma\tau} \quad (3.4)$$

for a system without internal torques [19–21]. For a central force system the isothermal elastic stiffness coefficients can be calculated from [19]

$$\begin{aligned}
c_{\alpha\beta\sigma\tau} = & \frac{1}{A} \left\langle \sum_{i<j} \Delta x_\alpha(ij) \Delta x_\beta(ij) \Delta x_\sigma(ij) \Delta x_\tau(ij) \frac{1}{r^2} \left(\Phi'' - \frac{\Phi'}{r} \right) \right\rangle \\
& - \frac{1}{k_B T A} \left\langle \delta \left(\sum_{i<j} \Delta x_\alpha(ij) \Delta x_\beta(ij) \frac{\Phi'}{r} \right) \delta \left(\sum_{i<j} \Delta x_\sigma(ij) \Delta x_\tau(ij) \frac{\Phi'}{r} \right) \right\rangle - \frac{1}{2A} \left\langle 2 \left\langle \sum_{i<j} \Delta x_\alpha(ij) \Delta x_\beta(ij) \frac{\Phi'}{r} \right\rangle \delta_{\sigma\tau} \right. \\
& - \left\langle \sum_{i<j} \Delta x_\alpha(ij) \Delta x_\sigma(ij) \frac{\Phi'}{r} \right\rangle \delta_{\beta\tau} - \left\langle \sum_{i<j} \Delta x_\alpha(ij) \Delta x_\tau(ij) \frac{\Phi'}{r} \right\rangle \delta_{\beta\sigma} - \left\langle \sum_{i<j} \Delta x_\beta(ij) \Delta x_\tau(ij) \frac{\Phi'}{r} \right\rangle \delta_{\alpha\sigma} \\
& \left. - \left\langle \sum_{i<j} \Delta x_\beta(ij) \Delta x_\sigma(ij) \frac{\Phi'}{r} \right\rangle \delta_{\alpha\tau} \right\rangle + \frac{N k_B T}{A} \delta_{\alpha\beta} \delta_{\sigma\tau}. \tag{3.5}
\end{aligned}$$

The stress tensor is given by

$$S_{\alpha\beta} = \frac{1}{A} \left\langle \sum_{i<j} \Delta x_\alpha(ij) \Delta x_\beta(ij) \frac{\Phi'}{r} \right\rangle - \frac{N k_B T}{A} \delta_{\alpha\beta}, \tag{3.6}$$

where the $\langle \dots \rangle$ designate configurational averages and $\delta(X) = X - \langle X \rangle$, $\Delta x_\alpha(ij)$ and r are defined as

$$\Delta x_\alpha(ij) = x_\alpha(i) - x_\alpha(j), \tag{3.7}$$

$$r^2 = |\Delta x_\alpha(ij)|^2. \tag{3.8}$$

A represents the area of the system. The first term in Eq. (3.5) is referred to as the ‘‘Born term.’’ It is the only nonzero term for homogeneous materials at zero temperature and in the absence of stress. The second term is the ‘‘fluctuation term’’ and is always negative. The third term is the ‘‘stress term.’’ The last is sometimes called the ‘‘kinetic term’’ [22]. We should emphasize that the area A which appears in Eqs. (3.5) and (3.6) must be the current (stressed) one [19], instead of the area of the stress-free state. The EFM provides a way to obtain all elastic constants from a single run and has the advantage that no actual deformations are made, so no symmetry breaking occurs. The EFM has been successfully applied to crystalline materials [22–24] and to soft materials such as crosslinked polymer melts and diluted lattice networks [15,25].

Exact values of the elastic constants at finite temperature are not usually available. However, the two methods should yield the same value. Hence, we can define the correct values of the shear modulus as the common limit of μ_{ss} and μ_{ef} .

IV. THE SYSTEM STUDIED

The system studied is the 2D diluted central force network, which has been used to show that the onset of mechanical rigidity occurs at a concentration of bonds and sites which is significantly larger than the percolation threshold [26]. It is simply a triangular network of springs of equal equilibrium length r_0 which is diluted by removing sites or bonds randomly. In this system, the nearest neighbors interact via the circularly symmetric potential $V_{nn}(r_{ij}) = \frac{1}{2}k(r_{ij} - r_0)^2$ and more distant neighbors are noninteracting. For this system, geometric percolation occurs at a concentration of sites $p_c = 0.5$ and rigidity percolation (at $T=0$) at p_r

≈ 0.6975 [26]. From here on p will mean the site concentration. The regime of interest for this study is the interval $p_c < p < p_r$ where, at zero temperature, the system is not rigid, but at finite temperature develops a finite shear modulus of entropic origin whose onset is p_c [18]. The unit of time is $t_0 = \sqrt{m/k}$ and the unit of temperature kr_0^2/k_B . The size of the system in most of our work is 16×16 sites. Systems of size 32×32 were also studied, but the results do not change our conclusions. The simulations were done with periodic boundary conditions at a temperature $T = 0.005kr_0^2/k_B$. We imposed a pure shear deformation $L_x \rightarrow \lambda L_x$ and $L_y \rightarrow L_y/\lambda$, where L_x and L_y are the lengths of the cell along the two Cartesian coordinate axes. So by definition for a small deformation $\eta_{11} = \lambda - 1$. We chose $\lambda = 1.001$ for $p \geq 0.85$ for safety. At low concentration, we chose $\lambda = 1.01$ in most situations.

To investigate the possibility of ergodicity breaking, we monitored for some samples the behavior of the variance and the skewness of the temperature distribution as was done in Refs. [27,28] for the Brownian dynamics algorithm. In the canonical ensemble, we should have with $\delta\mathcal{T}_{\text{int}} = \mathcal{T}_{\text{int}} - T$ [27]:

$$\text{variance } R_{\text{var}} \equiv \frac{Nd \langle (\delta\mathcal{T}_{\text{int}})^2 \rangle}{2 \langle \mathcal{T}_{\text{int}} \rangle^2} = 1, \tag{4.1}$$

$$\text{skewness } R_{\text{skew}} \equiv \frac{\sqrt{Nd} \langle (\delta\mathcal{T}_{\text{int}})^3 \rangle}{\sqrt{8} \langle (\delta\mathcal{T}_{\text{int}})^2 \rangle^{3/2}} = 1, \tag{4.2}$$

$$\text{with } \mathcal{T}_{\text{int}} = \frac{1}{d(N-1)k_B} \sum_{i=1}^N \frac{p_i^2}{m_i}. \tag{4.3}$$

Note that there is a slight difference between Eqs. (2.2) and (4.3) because the temperature is allowed to fluctuate in the Brownian dynamics algorithm. The violation of Eqs. (4.1) and (4.2) would indicate ergodicity breaking.

The shear modulus of the perfect triangular lattice at zero temperature and hydrostatic pressure is given exactly by $\mu \equiv C_{44} = \sqrt{3}/4(4 - 3r_0/a)k$ [19,29], where a is the lattice constant. $\mu = \sqrt{3}/4k = 0.433013k$ for $a = r_0$.

The nonbreakable bonds of the system introduce a set of quenched random variables. From the perspective of the present calculations, the most important effect of the quenched random variables is that it is necessary to average

TABLE I. Our best values of the average elastic modulus μ for pure shear deformation for 16×16 two-dimensional site diluted triangular lattices, with nearest neighbor linear restoring forces, in units of the force constant k , at $T = 0.005kr_0^2/k_B$, and with periodic boundary conditions (p is the site occupancy probability).

p	μ (units of k)
1	0.4332 ± 0.0002
0.85	0.1857 ± 0.0014
0.6	0.00859 ± 0.00006
0.51	0.00127 ± 0.00002
0.5	0.00

measured quantities over different realizations of the same concentration. At high concentration of sites ($p > 0.8$), 10–30 samples are enough to give high accurate results. However, at low concentration ($p \leq 0.60$) typically more than 250 samples are required and the lower the concentration, the larger the number of samples. The rule to choose the number of samples for those converged results in this work is that by increasing the number of samples, the uncertainty in the average results is about 3%, in a range of about 100 samples. In contrast, for those nonconverged results, 50–100 samples are in general enough to provide a clear answer as to whether convergence will occur. On the other hand, the strong fluctuations in the system at low density make convergence very slow and so fairly long running times are required. At high density ($p > 0.8$), 10^5 time steps are in general enough to get good convergence. But at low density, it requires in general 1–2 million time steps and we ran most of our samples up to 2 million time steps.

To facilitate the reading of the presentation of the results that follows, Table I gives our best values for μ for the 16×16 system at the four values of p that were used as tests of the algorithms: 1, 0.85, 0.6, and 0.51. These four values cover the whole range from crystalline to disordered and very soft. $p = 0.5$ is the percolation threshold, at which $\mu = 0$.

V. RESULTS

A. Algorithm A: The velocity rescaling scheme

The results for algorithm A have been given in Ref. [15]. In summary, at high density, good agreement between μ_{ss} and μ_{ef} is obtained for the time step $\Delta t = 0.05t_0$. For instance, at density $p = 0.85$, $\mu_{ss} = 0.1846k$, and $\mu_{ef} = 0.1870k$. However, at low density where the entropy is significant, even a much smaller time step, $\Delta t = 0.005t_0$, did not give convergent results. This is the case, for instance, at the density $p = 0.6$, where μ_{ef} and μ_{ss} have different trends, as shown in Fig. 1(a). Good agreement was obtained with $\Delta t = 0.0016t_0$ [see Fig. 1(b)]. After an extrapolation using $\mu(t) = \mu(\infty) + a/t$, we found $\mu_{ef} = \mu_{ef}(\infty) = 0.00865k$ and $\mu_{ss} = 0.00878k$. The agreement between μ_{ef} and μ_{ss} improved with increasing number of samples. Figure 2 shows clearly that μ_{ef} and μ_{ss} go to a common limit when the time step is decreased.

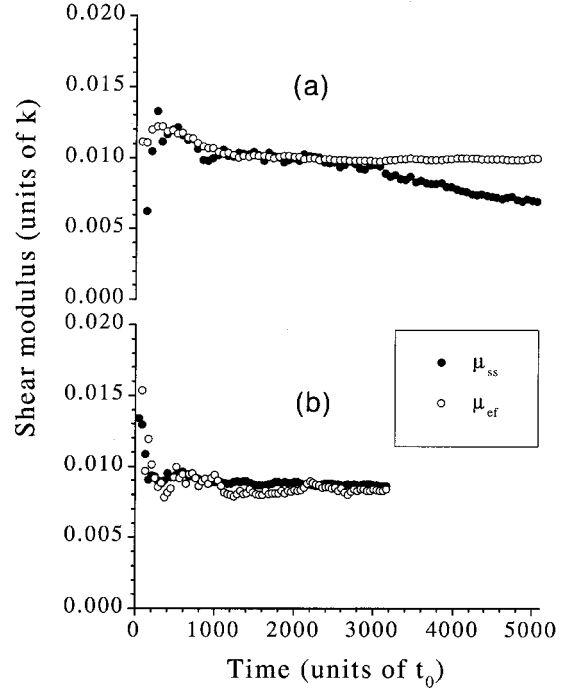


FIG. 1. Algorithm A: velocity rescaling scheme. (a) Average μ_{ss} and μ_{ef} for 150 samples vs time at $p = 0.6$. Total running time: 10^6 time steps with $\Delta t = 0.005t_0$. (b) Average μ_{ss} and μ_{ef} for 260 samples vs time at $p = 0.6$. Total running time: 2×10^6 time steps with $\Delta t = 0.0016t_0$.

B. Algorithm B: The damped force algorithm

In previously published work on dense systems, time steps typically of the order of $\Delta t = 0.1t_0$ to $\Delta t = 0.05t_0$ have been used [25,30,31]. In diluted systems at $p = 0.6$, with Δt

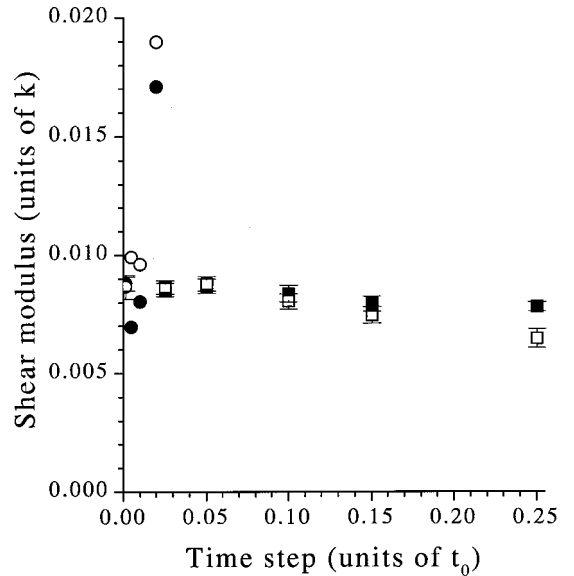


FIG. 2. Average μ_{ss} (solid symbols) and μ_{ef} (open symbols) with error bars vs time step for the velocity rescaling scheme (circles) (Algorithm A) and the rigorous Brownian dynamics algorithm (squares) (Algorithm C) at $p = 0.6$. We do not plot error bars for the nonconverged data. The latter are limited to the very small time step values with convergence for $\Delta = 0.0016t_0$, the only velocity rescaling data point with an error bar.

$=0.02t_0$, we get $\mu_{ef} \approx 0.00824k$ and $\mu_{ss} \approx 0.00839k$. It is much better than what was obtained using A, in which both μ_{ef} and μ_{ss} diverge at the same Δt , but it is not good enough. Therefore, we reduced the time step to $\Delta t = 0.005t_0$ and got $\mu_{ef} = 0.00852k$ and $\mu_{ss} = 0.00840k$.

However, at $p = 0.51$, using $\Delta t = 0.005t_0$ we found again a large disagreement between $\mu_{ss} (=0.00128k)$ and $\mu_{ef} (=0.00243k)$ though both of them converged well. Reducing the time step further to $\Delta t = 0.0016t_0$, we got $\mu_{ss} = 0.00128k$ but $\mu_{ef} = 0.00360k$. Note that μ_{ss} agrees well with the value obtained from C (see next section) but μ_{ef} is overestimated, as with D (see Sec. V D) at higher density ($p = 0.85$). Also we can note that reducing Δt further did not reduce the gap between μ_{ss} and μ_{ef} .

C. Algorithm C: The rigorous Brownian dynamics algorithm

The very low efficiency and the likely failure of algorithms A and B in the critical regime stimulated us to try the rigorous method C. First, we found that using C, the variance of the temperature satisfied Eq. (4.1) to within 1% in 50 000 time steps and the skewness satisfied Eq. (4.2) to within 5% in 100 000 time steps for every realization at $p = 0.6$. Δt was equal to $0.05t_0$ and the equilibration time to 20 000 time steps. The uncertainty in $\langle T_{int} \rangle$ itself is stabilized to $< 5/1000$ within a few thousand time steps even with $\Delta t = 0.25t_0$. Averaging over many samples would yield an even better agreement. Therefore, there was no evidence of ergodicity breaking in this system.

For $p = 1$, $\Delta t = 0.25t_0$ still gives almost perfect results. We found that $\mu_{ef} = 0.4332k$ and $\mu_{ss} = 0.4333k$ up to 10^5 time steps. At $p = 0.85$, using $\Delta t = 0.05t_0$, we found that $\mu_{ef} = 0.1843k$ and $\mu_{ss} = 0.1871k$. These values agree well with the results of algorithm A. Moreover, we found that at $p = 0.6$, from $\Delta t = 0.25t_0$ to $0.025t_0$, the uncertainty in the total energy and in the pressure, which are, respectively, $< 0.1\%$ and $< 3\%$, showed no significant change in a single realization. μ_{ef} and μ_{ss} vs time steps at $p = 0.6$ are also shown in Fig. 2.

Again, we find clearly that μ_{ef} and μ_{ss} go to a common limit with decreasing time step. Using $\Delta t = 0.25t_0$, both μ_{ss} and μ_{ef} converged well but to clearly different limits, $\mu_{ef} = 0.00648k$ and $\mu_{ss} = 0.00781k$, as shown in curves (a) and (b) of Fig. 3. At $\Delta t = 0.15t_0$, the agreement is improved greatly but the limits are still clearly different: $\mu_{ef} = 0.00746k$ and $\mu_{ss} = 0.00794k$. The relative difference is greater than 6% and does not decrease with increasing number of samples. At $\Delta t = 0.1t_0$, the agreement is improved further, but we can still observe different trends: $\mu_{ef} = 0.00804k$ and $\mu_{ss} = 0.00836k$. However, at $\Delta t = 0.05t_0$, we got $\mu_{ef} = 0.00879k$ and $\mu_{ss} = 0.00868k$. These values agree well with the results from the velocity rescaling and the damped force algorithms. The results as shown in curves (c) and (d) of Fig. 3, show a clear trend towards a common limit. Using $\Delta t = 0.025t_0$, we got $\mu_{ef} = 0.00865k$ and $\mu_{ss} = 0.00853k$, values close to those obtained with $\Delta t = 0.05t_0$. We also found that with $\Delta t = 0.05t_0$ and $\Delta t = 0.025t_0$, 20 samples are enough to show good agreement between μ_{ef} and μ_{ss} . But to get an accurate result, i.e., a convergent result with $\approx 3\%$ accuracy and little change with increasing number of samples, requires about 140 samples at both time

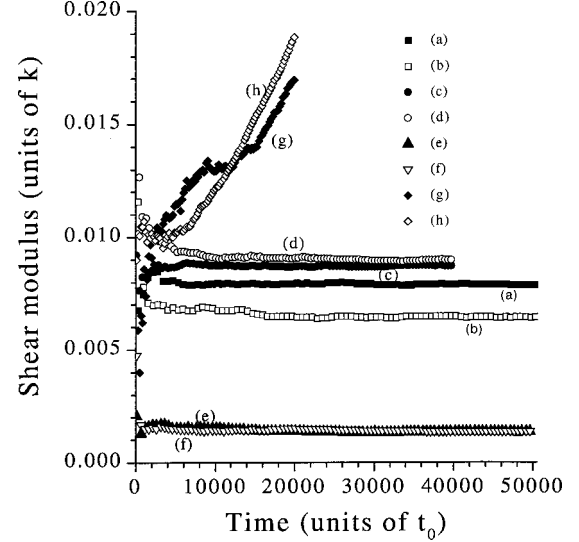


FIG. 3. Algorithm C: rigorous Brownian dynamics [curves (a) to (f)]. Algorithm A: velocity rescaling scheme [curves (g) and (h)]. As a rule μ_{ss} have solid symbols and μ_{ef} open symbols. Algorithm C. Curve (a) is the average μ_{ss} for 160 samples vs time at $p = 0.60$. Total running time: 5×10^5 time steps with $\Delta t = 0.25t_0$. The portion from $50000t_0$ to $125000t_0$ is not shown because both μ_{ss} and μ_{ef} are essentially constant. Curve (b) is the average μ_{ef} corresponding to (a). Curve (c) is the average μ_{ss} for 260 samples vs time going up to 8×10^5 time steps at $p = 0.60$ with $\Delta t = 0.05t_0$. Curve (d) is the average μ_{ef} corresponding to (c). Curve (e) is the average μ_{ss} for 360 samples vs time for up to 10^6 time steps at $p = 0.51$. $\Delta t = 0.05t_0$. Curve (f) is the average μ_{ef} corresponding to (e). Algorithm A. Curve (g) is the average μ_{ss} for 50 samples vs time up to 10^6 time steps at $p = 0.60$. $\Delta t = 0.02t_0$. Curve (h) is the average μ_{ef} corresponding to (g).

steps. The properly converging sequences of μ_{ef} and μ_{ss} vs time steps at this value of $p = 0.6$ are shown in Fig. 2.

These results support further the conclusion that the allowable Δt should be smaller than the value which stabilizes the total energy and pressure or the value required in the perfect lattice [15]. Moreover, the optimum time step is significantly larger than for the previous two algorithms, compensating for the slowness of the computer algorithm.

To explore whether the time step is sensitive to the density for this algorithm and whether it is possible to make μ_{ss} agree with μ_{ef} in all regimes, we carried out simulations at $p = 0.51$. We found that using $\Delta t = 0.1t_0$ the agreement between the two methods is not satisfactory, $\mu_{ef} \approx 0.00126k$ but $\mu_{ss} \approx 0.00142k$, and the gap does not decrease with an increase in the number of samples. However, with $\Delta t = 0.05t_0$, the agreement is good, $\mu_{ef} = 0.00126k$ and $\mu_{ss} = 0.00129k$ as shown in curves (e) and (f) of Fig. 3, and the results were stable with 240 samples. The number of samples required for a good result is significantly larger than at $p = 0.6$ (≈ 140). The correlation length increases rapidly with decreasing p . The agreement at $p = 0.51$ is remarkable considering that the shear modulus at this density is very small.

We can therefore conclude that the rigorous Brownian dynamics algorithm guarantees correct μ_{ss} and μ_{ef} values, and the time step is not sensitive to the density of sites in the system. We found however that a reasonable deformation may be necessary for convergence, especially for μ_{ss} . At

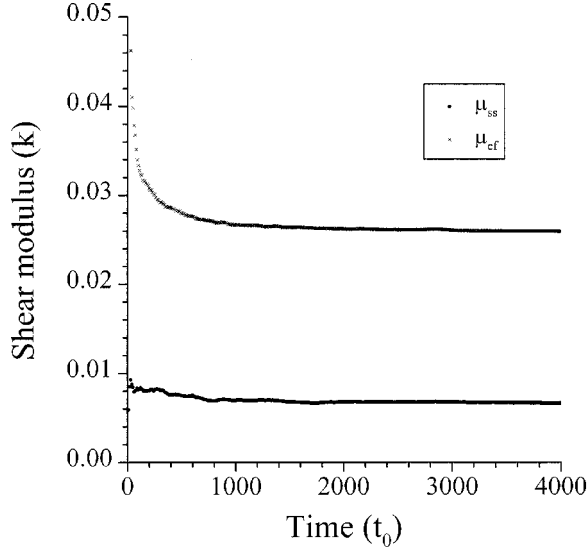


FIG. 4. Algorithm D: Approximate Brownian dynamics. Average μ_{ss} and μ_{ef} for 300 samples vs time up to 2×10^6 time steps at $p=0.6$. $\Delta t=0.002t_0$.

$p=0.6$, with a very small deformation $\lambda=1.001$, proper equilibration was very slow. Even using a rather small time step $\Delta t=0.01t_0$, μ_{ss} is not convergent and $\mu_{ef}=0.00804k$ is obviously smaller than it should be.

D. Algorithm D: The approximate Brownian dynamics

Historically this is the first method we used to calculate elastic constants in the DCFN and the serious discrepancy between μ_{ss} and μ_{ef} found with this method led us to try other methods. At $p=1$ with $\Delta t=0.01t_0$, we found that $\mu_{ss}=0.4318k$, $\mu_{ef}=0.4293k$. The agreement between μ_{ss} and μ_{ef} is still rather good though not as good as with the rigorous algorithm C. However, an obvious discrepancy appears once $p < 1$. At $p=0.85$ with $\Delta t=0.001t_0$, we got $\mu_{ss}=0.1864k$ but $\mu_{ef}=0.2187k$. It is interesting to note that μ_{ss} is still rather good but μ_{ef} is obviously too large, similar to the result obtained from algorithm B at $p=0.51$. However, at $p=0.6$, $\Delta t=0.002t_0$, we got $\mu_{ss}=0.0066k$ and $\mu_{ef}=0.0270k$. We can see from Fig. 4 that both μ_{ss} and μ_{ef} converge well but to a different limit. Comparing with the results from the three other algorithms, we can see that this method overestimates μ_{ef} but underestimates μ_{ss} at low p . From the similarity between the results of B at $p=0.51$ and those of this algorithm at $p=0.85$, it is reasonable to think that the source of the problem may be intrinsically the same, and that it is ergodicity breaking. The same may apply to algorithm A.

With D, the temperature stabilizes to the required temperature within a few thousand time steps for *every* realization. However, in contrast to C, both the variance and the skewness seriously violate Eqs. (4.1) and (4.2) even at $p=1.0$. At $p=1.0$, the discrepancy for the variance from Eq. (4.1) can be as large as 50% and for the skewness it is about 30%, even after averaging over 40 samples [see Figs. 5(a) and 5(b)]. At $p=0.6$, the discrepancy for the variance can also be about 25% and for the skewness about 22%, as shown in Figs. 5(c) and 5(d). Moreover, we observed systematic asymmetries in $K_x = \langle \sum (p_x^2/2m) \rangle$ and K_y

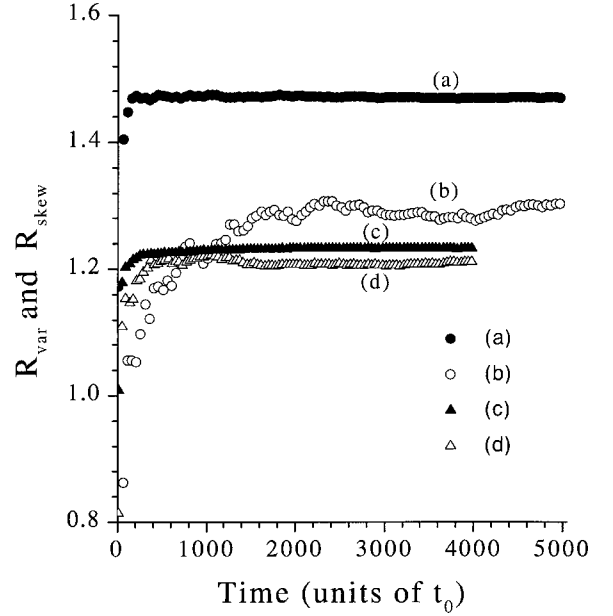


FIG. 5. Algorithm D: Approximate Brownian dynamics. Curve (a) is the average of R_{var} for 40 samples vs time up to 10^6 time steps at $p=1$ with $\Delta t=0.01t_0$. Curve (b) is the average of R_{skew} corresponding to curve (a). Curve (c) is the average of R_{var} for 300 samples vs time up to 2×10^6 time steps at $p=0.6$ with $\Delta t=0.002t_0$. Curve (d) is the average of R_{skew} corresponding to curve (c).

$= \langle \sum (p_y^2/2m) \rangle$ even for the undeformed perfect lattice. A and B work better because they at least generate correct canonical distributions in the configuration space.

VI. DISCUSSION AND CONCLUSION

As it should be, the two methods to calculate the elastic constants, the macroscopic measurement μ_{ss} and the microscopic measurement μ_{ef} , can be made to agree if we choose the proper time step and/or the proper simulation algorithm. From the results obtained in the above section and by choosing the shear modulus as the common limit of μ_{ss} and μ_{ef} , we can obtain reliable and accurate values (see Table I). We may recall that convergence of one of the quantities is not in itself a reliable measure of accuracy, as the limit could be wrong.

The first factor affecting the convergence of μ_{ef} and μ_{ss} is the time step. Our present results confirm our earlier discovery [15] that the usual criteria for the choice of the time step, i.e., the stabilities of the energy and the pressure are not always sufficient to ensure a faithful simulation of the properties of a system. The optimum time step for soft materials can be much smaller than for a rigid material. This can be explained by the fact that in the very inhomogeneous soft regime (highly diluted lattice) changes in configuration may require passage from one metastable state to another with some particles going through saddle points. These particles may require a smaller Δt and they determine the maximum Δt allowed for the whole system. We found that as we decrease Δt , all types of convergence situations are observed for μ_{ef} and μ_{ss} . First, neither μ_{ss} nor μ_{ef} converge, corresponding to a far too large Δt , as shown in curves (g) and (h) of Fig. 3. Secondly, one quantity converges but the other

does not, as shown in Fig. 1(a). The next possibility is that both μ_{ss} and μ_{ef} converge but not to a common limit, as shown in curves (a) and (b) of Figs. 3 and 4. Finally, both μ_{ss} and μ_{ef} converge to a common limit. We found that once a common limit is achieved, increasing the number of samples may improve the accuracy but reducing Δt further gives little improvement. This makes us conclude that the agreement between μ_{ef} and μ_{ss} can be used as a criterion to choose the proper time step and/or proper simulation method. This criterion is computationally efficient since both μ_{ef} and μ_{ss} can be calculated simultaneously in the same run as mentioned in Sec. III.

The optimum Δt is algorithm sensitive and can differ by an order of magnitude from one algorithm to the other. It should not be surprising that the rigorous Brownian dynamics algorithm C allows a large time step. The key to implementing C is to realize a proper distribution of the random force [12], and this distribution should be dependent more on the number of samplings (i.e., the running time in MD) than on the time step. The corresponding random variables which appear in the numerical integration of the equations of motion are of the order of $\mathcal{O}(\Delta t^2)$, so they dominate the cut off and round off errors in a rather large range of time steps. In other words, the contact with the heat bath helps to stabilize the system. Although for the same total number of steps, C requires a computational time 2 to 3 times longer than algorithms A and B (velocity rescaling and damped force, respectively), its 10 to 30 times larger time step allows for better efficiency, not to mention the increased confidence that this algorithm provides. In contrast, of all the ways to realize a canonical ensemble, A may require the smallest Δt because it does not deal with the coordinates and the velocities in parallel, so some uncorrelated disturbances may be added to the integral of the equations of motion.

The same problem also exists in the microcanonical ensemble. For the system with $p=0.6$ and $\lambda=1.01$ and using the velocity Verlet algorithm [12] to integrate the equations of motion, we found that with Δt from $0.05t_0$ to $0.02t_0$, the uncertainty in the total energy and pressure remains almost the same. However, at $\Delta t=0.05t_0$, μ_{ef} and μ_{ss} converge to different limits; $\mu_{ef}=0.00940k$ and $\mu_{ss}=0.00806k$ with 260 samples. The increase in the number of samples does not reduce the gap between μ_{ef} and μ_{ss} . In contrast, with $\Delta t=0.02t_0$, we get $\mu_{ef}=0.00844k$ and $\mu_{ss}=0.00824k$ from 300 samples, a rather good agreement again and very close to the values obtained from the Brownian dynamics.

The second factor affecting the convergence of μ_{ef} and μ_{ss} is the choice of the simulation algorithm. We found that for soft inhomogeneous materials it should be necessary to implement the rigorous canonical ensemble to study *most* properties. The approximate algorithms cannot guarantee the correctness of the results even though they can converge

well. Our results show that for the DCFN in the soft regime, the approximate Brownian dynamics algorithm D fails to give correct results for both μ_{ef} and μ_{ss} . A and B fail for μ_{ef} at low density, but they can give correct μ_{ss} even at rather low density. Therefore, A and B perform better than D but not as well as C. The reliability of A and B decreases however as the material becomes softer, as ever smaller time steps are required to maintain agreement between μ_{ss} and μ_{ef} . This is not a satisfactory or reassuring situation.

The problem with the approximate algorithms must result from ergodicity breaking. In the rigid regime, ergodicity breaking has little effect on the result since there is a sharp minimum in the free energy in phase space and most parts of the phase space give a zero contribution to the ensemble average. The same seems to hold true for liquids for the opposite reason, a homogeneous distribution of states in phase space. However, for a soft inhomogeneous material, there may exist a large number of configurations close in energy which need to be sampled with the correct statistical weight, and therefore the effect of ergodicity breaking becomes non-negligible. For algorithms A and B, the potential energy can fluctuate but the temperature cannot as measured by the total kinetic energy. The dynamics of the collisions of the chains with each other may not be well represented and hence the entropy would not be correct. And algorithm D, although it keeps the temperature fairly constant, has too large a variance and skewness, and hence makes a rather poor canonical ensemble.

It is not yet clear why μ_{ss} is always better than μ_{ef} in the approximate methods for the two systems that we have studied, the DCFN and the cross-linked polymer melts [14,15]. One possible explanation is that μ_{ef} is a direct second derivative of the free energy, so it requires a correct representation of the detailed structure of the phase space, and hence is more sensitive to ergodicity breaking. The difficulties encountered with the shear modulus must occur for other response functions as well, such as the specific heat.

In conclusion, this work demonstrates the importance of realizing a rigorous canonical ensemble for inhomogeneous soft materials. Similar problems may also occur in the approximate constant T and constant pressure MD simulations. There are at least three other rigorous ways to realize the canonical ensemble in MD simulations [4,10,11]. The appeal of Brownian dynamics for high entropy systems is its use of random numbers which permits an efficient sampling of the available phase space.

ACKNOWLEDGMENTS

This work was supported by the Natural Sciences and Engineering Research Council of Canada. Stimulating discussions with Michael Plischke and Dan Vernon are gratefully acknowledged.

[1] L.V. Woodcock, Chem. Phys. Lett. **10**, 257 (1971).
 [2] W.T. Ashurst and W.G. Hoover, Phys. Rev. Lett. **31**, 206 (1973).
 [3] D.L. Ermak, (unpublished); D.L. Ermak and H. Buckholtz, J. Comput. Phys. **35**, 169 (1980).

[4] H.C. Andersen, J. Chem. Phys. **72**, 2384 (1980).
 [5] W.G. Hoover, A.J.C. Ladd, and B. Moran, Phys. Rev. Lett. **48**, 1818 (1982).
 [6] W. Hoover, Physica A **118**, 111 (1983).
 [7] D.J. Evans and G.P. Morriss, Chem. Phys. **77**, 63 (1983);

- Phys. Lett. **98A**, 433 (1983).
- [8] J.M. Haile and S. Gupta, J. Chem. Phys. **79**, 3067 (1983).
- [9] H.J.C. Berendsen, J.P.M. Postma, W.F. van Gunsteren, A. Di-Nola, and J.R. Haak, J. Chem. Phys. **81**, 3684 (1984).
- [10] S. Nosé, Mol. Phys. **52**, 255 (1984); J. Chem. Phys. **81**, 511 (1984).
- [11] W.G. Hoover, Phys. Rev. A **31**, 1695 (1985).
- [12] M.P. Allen and D.J. Tildesley, *Computer Simulation of Liquids* (Oxford University Press, New York, 1987).
- [13] J. M. Haile, *Molecular Dynamics Simulation* (Wiley, Toronto, 1992).
- [14] S.J. Barsky, M. Plischke, B. Joós, and Z. Zhou, Phys. Rev. E **54**, 5370 (1996).
- [15] Z. Zhou and B. Joós, Modell. Simul. Mater. Sci. Eng. **7**, 383 (1999).
- [16] D. Brown and J.H.R. Clarke, Mol. Phys. **51**, 1243 (1984).
- [17] E.R. Duering, K. Kremer, and G.S. Grest, J. Chem. Phys. **101**, 8169 (1994).
- [18] M. Plischke and B. Joós, Phys. Rev. Lett. **80**, 4907 (1998).
- [19] Z. Zhou and B. Joós, Phys. Rev. B **54**, 3841 (1996).
- [20] J. Wang, S. Yip, S.R. Phillpot, and D. Wolf, Phys. Rev. Lett. **71**, 4182 (1993); J. Wang, J. Li, S. Yip, S. Phillpot, and D. Wolf, Phys. Rev. B **52**, 12 627 (1995).
- [21] T.H.K. Barron and M.L. Klein, Proc. Phys. Soc. London **85**, 523 (1965).
- [22] D.R. Squire, A.C. Holt, and W.G. Hoover, Physica (Amsterdam) **42**, 388 (1969).
- [23] J.R. Ray, M.C. Moody, and A. Rahman, Phys. Rev. B **32**, 733 (1985).
- [24] J.R. Ray, M.C. Moody, and A. Rahman, Phys. Rev. B **33**, 895 (1986).
- [25] B. Joós, Z. Zhou, and M.S. Duesbery, Phys. Rev. B **50**, 8763 (1994).
- [26] D.J. Jacobs and M.F. Thorpe, Phys. Rev. Lett. **75**, 4051 (1995); D.J. Jacobs and M.F. Thorpe, Phys. Rev. E **53**, 3682 (1996); C. Moukarzel and P.M. Duxbury, Phys. Rev. Lett. **75**, 4055 (1995).
- [27] B.L. Holian, A.F. Voter, and R. Ravelo, Phys. Rev. E **52**, 2338 (1995).
- [28] R. Simonazzi and A. Tenenbaum, Phys. Rev. E **54**, 964 (1996).
- [29] Z. Zhou and B. Joós, Phys. Rev. B **56**, 2997 (1997).
- [30] J.A. Combs, Phys. Rev. Lett. **61**, 714 (1988); Phys. Rev. B **38**, 6751 (1988).
- [31] Z. Zhou and B. Joós, Surf. Sci. **323**, 311 (1995).